Published in final edited form as:
Comput Methods Biomech Biomed Eng Imaging Vis. 2014 ; 2(4): 217–222. doi: 10.1080/21681163.2013.851627.

Speech function of the oropharyngeal isthmus: A modeling study

Bryan Gick[1,2], **Peter Anderson**[3], **Hui Chen**[3], **Chenhao Chiu**[1], **Ho Beom Kwon**[4], **Ian Stavness**[5], **Ling Tsou**[3], and **Sidney Fels**[3]

[1]Department of Linguistics, University of British Columbia

[2]Haskins Laboratories, New Haven, CT

[3]Department of Electrical and Computer Engineering, University of British Columbia

[4]Department of Prosthodontics, School of Dentistry, Seoul National University

[5]Department of Computer Science, University of Saskatchewan

Abstract

A finite element method (FEM) based numerical model of upper airway structures (jaw, tongue, maxilla, soft palate) was implemented to observe interactions between the soft palate and tongue, and in particular to distinguish the contributions of individual muscles in producing speech-relevant constrictions of the oropharyngeal isthmus (OPI), or “uvular” region of the oral tract. Simulations revealed a sphincter-like general operation for the OPI, particularly with regard to the function of the palatoglossus muscle. Further, as has been observed with the lips, the OPI can be controlled by multiple distinct muscular mechanisms, each reliably producing a different sized opening and robust to activation noise, suggestive of a modular view of speech motor control. As off-midline structures of the OPI are difficult to observe during speech production, biomechanical simulation offers a promising approach to studying these structures.

Introduction

The tongue and the soft palate have separately received much attention in their respective roles of forming oral constrictions and of opening and closing the velopharyngeal port. However, comparatively little consideration has been given to the combined action of these structures in producing constrictions of the oropharyngeal isthmus (OPI), the narrowing in the region of the faucial pillars that separates the oral and pharyngeal spaces of the vocal tract (see Figure 1). Contrary to the received view of OPI constrictions in oral speech sounds (e.g., dorsal sounds such as the French /r/ or English /w/) being effected primarily through raising and retraction of the tongue, Gick et al. (2013) identify a posterior portion of the soft palate that contributes actively to oral constrictions in Québec French; this contribution of the “velic traverse” (the “veil” from which the velum, or soft palate, derives its name) suggests that the entire OPI may function rather like the lips, with sphincter-like

Corresponding author information: Bryan Gick, Department of Linguistics, 2613 West Mall, Vancouver, BC V6T1Z4, Canada, gick@mail.ubc.ca.

constrictions converging from all sides. This proposal is consistent with Kuehn and Azzam's (1978) observation that OPI constrictions may (in principle) be produced by one of several distinct mechanisms: raising the tongue, lowering the velum, or narrowing the faucial pillars. Testing this proposal, however, has been challenging, as the off-midline structures of the OPI rotate and translate in and out of plane during speech, making them difficult to observe using standard imaging tools. Biomechanical simulation offers an alternative approach to studying the speech function of these OPI structures.

Of the many muscles that are in a position to contribute to OPI constriction, the palatoglossus (PG) muscle is of particular interest, as it forms an almost complete ring running through the whole OPI, making PG the primary single muscle of the OPI (cf. the "glossopalatine sphincter" described in the swallowing literature; Faber 1878:114; Dantas et al. 1990). Activity of the PG muscle in speech has been widely viewed as contributing both to elevating the tongue to produce oral constrictions, and to lowering the velum to open the velopharyngeal port for nasal sounds (e.g., Fritzell 1969; Lubker et al. 1970; Benguerel et al. 1977, Campos et al. 2012). However, the relationship between PG activity and tongue and velum movements has been found to vary greatly across individuals, languages, phonetic contexts, and studies (e.g., Bell-Berti and Hirose 1973; Lubker and May 1973; Bell-Berti 1976; Moon et al., 1994). This unreliable relationship between PG activity and tongue raising is not surprising, as the PG's small diameter, large amount of connective tissue, and non-rigid attachment location make a significant tongue-raising function implausible for most speakers (Kuehn and Azzam, 1978: 356–358), and as extrinsic muscles such as PG appear to be unnecessary for tongue raising and backing movements, which can be achieved through intrinsic hydrostatics (Takano and Honda 2007). Some researchers have suggested a more generalized function for PG of reducing the area of the OPI, potentially including narrowing of the space between the anterior faucial pillars (see reviews by Fritzell 1979; Perry 2011) in addition to tongue elevation and velum lowering. Further to this point, we predict that PG will exhibit an initial phase of narrowing the OPI, as the pillars must first become taut before they can exert any substantial downward force on the velum or upward force on the tongue. Our simulations will thus first test for this phased effect of PG activation, starting with a narrowing phase and followed by a multi-directional constriction, in a model with biomechanically realistic coupling between the tongue and soft palate.

Second, contrary to the predominantly downward vectors of the two inferior soft palate muscles, PG and palatopharyngeus (PP) (see Kuehn and Azzam 1978), Gick et al. (2013) observe a primarily forward (rather than downward) vector of the velic traverse or "veil" in OPI constrictions (note that this movement of the veil does not appear in their x-ray study to affect velopharyngeal port closure). What little has been said about the positioning of this inferior portion of the soft palate has been largely conjectural, but may suggest a mechanism involving coordination of the PG and PP muscles (Seaver and Kuehn 1980; Kuehn et al. 1982; Moon et al. 1994), and may further suggest a possible important role for the intrinsic posterior portion of PG, which courses anteroposteriorly within the soft palate (and would hence have the strongest potential for a forward pull on the veil. Thus, our simulations test for the relative contributions of anterior PG (PGa), posterior PG (PGp), and PP in constrictions of the OPI.

Methods

We implemented a numerical model of the upper airway including geometries of the jaw, tongue, hyoid bone, skull, and soft palate. Previous studies have reported FEM-based models of the soft palate (e.g., Berry et al. 1999; Chen et al. 2012) and the jaw–tongue–hyoid complex (e.g., Gerard et al. 2006; Stavness et al. 2011, 2012). The present work extends this work by extensively modifying the soft palate model of Chen et al. (2012), and fitting it to the jaw–tongue–hyoid model of Stavness et al. (2011, 2012), with the particular goal of observing interactions between the soft palate and tongue in the region of the OPI. The resulting combined model, built using Artisynth (www.artisynth.org), an open-source FEM simulation toolkit, is shown in Figure 2.

The initial soft palate geometry of Chen et al. (2012) was morphed with reference to the geometries of the skull, tongue, and surrounding structures. The initial morph was done algorithmically, but additional modifications were made by hand (such as enforcing symmetry to the midsagittal plane). The soft palate geometry from Serrurier and Badin (2008) provided a useful guide, though that geometry does not extend to all the regions we model in the present study. A tetrahedral volumetric mesh was constructed for the soft palate geometry using TetGen (www.tetgen.org).

The resulting soft palate model, shown in Figure 3, includes five muscle groups: palatoglossus (split into anterior and posterior parts), palatopharyngeus, musculus uvulae, tensor veli palatini, and levator veli palatini. Muscles were modeled using point-to-point Hill-type muscles that have non-linear force-length and force-velocity properties (Zajac 1989), with fiber path definitions based on geometry and known connection points on the skull and soft tissues. Muscles attached to a surrounding FEM mesh will directly apply forces to that mesh when activated, but can also extend outside of the mesh, and thus provide a way to anchor the soft palate to other geometries. In this way, the origins of levator veli palatini (LVP) and tensor veli palatini (TVP) muscles were anchored superiorly to fixed points (visible in Figure 2) on the skull, the anterior edge of the soft palate geometry was anchored anteriorly at the interface with the hard palate (visible in Figure 2), the palatopharyngeus muscle was anchored inferiorly to a hypothetical fixed origin point (visible in Figure 3) in the pharynx, and the palatoglossus muscle was anchored to dynamic insertion points on the tongue (visible in Figure 3), thus defining the coupling of the soft palate model to the rest of the model. To simulate the closed configuration of the velopharyngeal port observed in Gick et al. (2013), in addition to the constant resistance provided by LVP and TVP, elements medial to the LVP insertion points on the superior surface of the soft palate were fixed so as to approximate the palatal bulge visible in Serrurier and Badin (2008: 2347).

Muscle forces are defined by $F = F_{max} * EMG$ (Korioth and Hannam 1994; Peck et al. 2000), where F_{max} is the maximum force a muscle can produce and EMG is the muscle activation ($0 < EMG < 1$). F_{max} can be estimated as $F_{max} = A_{cs} * K$, where K is a constant typically taken to be 40 N/cm^2, and A_{cs} is the cross-sectional area. For example, taking the diameter of LVP to be 5.4 mm (Ettema et al. 2002), one can estimate that its maximum force is around 9 N; however, the exact value is not critical because it is scaled by activations typically around 0.1 in our simulations. Berry et al. (1999) reports muscle forces around 0.3N, supporting our estimate of forces less than 1N. In previous models lacking embedded muscles, the material of the soft palate has been modeled as a linear elastic material with Young's modulus E = 25,000 Pa (Wang et al. 2012; Liu et al. 2007; Huang et al. 2005). We also use a linear elastic model, but take a slightly softer E = 15,000 Pa, bearing in mind that the embedded muscles in our model will cause soft palate tissue to stiffen with activation (see, e.g., Cui et al. 2008).

To test our hypotheses concerning the general role of PG in OPI constriction, as well as its possible interactions with PP, we simulated activations of the anterior and posterior PG muscles and the PP muscles. Simulations were set to occur within a 750 ms window. No muscles were activated during the first 200 ms of this window to allow gravity to act upon the model, and muscle activations did not continue past 600 ms, allowing time for movements to resolve. OPI area was calculated using an intersect plane (visible in Figure 4), such that the plane intersected all relevant OPI structures. The area of this plane, bounded by points of intersection with the surrounding elements of the tongue, soft palate, and anterior faucial pillars, was calculated based on line-of-sight from a pre-defined point at each time step of 1 ms.

Results

The effect of simulated PGa activation is shown in the time-lapse sequence in Figure 4. As can be seen in the images, the initial phase from (4a) to (4b) consists of narrowing of the isthmus by medial compression of the anterior faucial pillars (note the width of the pillars relative to the intersecting grid) accompanied by greatly increased contact between the anterior pillars and the tongue; contributing to this effect is a small amount of tongue raising. The latter phase from (4b) to (4c) shows further "hugging" of the anterior pillars around the tongue, as well as a continued concomitant small amount of tongue raising and velum lowering.

While PGa activation alone produced no appreciable forward movement of the uvula, Figure 5 shows the effect of adding PGp activation on the position of the velic traverse/veil (and hence the uvula). In this simulation, the yellow line in (5b) clearly traces a predominantly forward rather than downward trajectory for the uvula under the influence of the posterior portion of the PG muscle.

Finally, OPI intersect plane areas are plotted in Figure 6, showing the contributions of the different groupings of PG and PP to the area of the OPI. Here we see that activating only PGa (indicated by the dashed line in Figure 6) produces a small, linear effect on overall OPI area. Adding PGp (dotted line) yields not only a dramatic increase in OPI constriction (as the addition of PGp causes the veil to shorten slightly and bend forward toward the tongue dorsum), but a strongly nonlinear effect, whereby the area of the constriction levels out at a threshold of roughly a third of the muscle activation range. The further addition of PP (solid line) results in a different nonlinear effect, having a similar activation threshold but leveling out at a much smaller (though still not fully closed) area of opening. PP acts as an antagonist to PG, preventing the veil from shortening during the activation of PGp, as well as narrowing the posterior pillars. For both nonlinear effects, additional muscle activation fails to close the OPI fully because of increased stiffness resulting from muscle activation and elasticity in the surrounding tissues.

Discussion

Our simulation results show that the OPI indeed constricts from all sides, particularly through activation of the PG, and to some extent, the PP muscle. However, it is the intrinsic posterior portion of the PG muscle that reshapes the traverse or "veil" of the soft palate, allowing it to angle forward toward the tongue, providing effective OPI constriction without compromising velopharyngeal port closure. These results thus begin to touch upon the function of the intrinsic portions of the muscles of the soft palate, of which little is known.

Further, we observe two distinct mechanisms for effecting OPI constrictions, each of which yields a different-sized opening. In this sense, OPI function indeed seems analogous to the lips, where discrete, task-specific mechanisms have been described as being used to produce different-sized constrictions; mechanisms of this kind, associated with distinct muscle combinations, have been described as producing biomechanically nonlinear or quantal-like effects (Fujimura 1989; Nazari et al. 2011; Gick et al. 2011) similar to those observed here for the OPI. Such effects have been used to explain why different lip shapes are associated with different areas (degrees) of constrictions in speech (e.g., flat-shaped lips for complete closures, but rounded, protruded lips for vowels; Gick et al. 2011).

The mechanisms observed here suggest that larger-area OPI constrictions (e.g., for vowels such as [u]) may be produced using a PG-based structure, while smaller-area (though not completely closed) constrictions (as in French /r/ or German uvular fricatives) may be produced using a structure combining activation of PG + PP. In the latter mechanism, PG pulls downward and forward while PP pulls downward and back, providing a "sling" effect that is capable of directing a stronger overall pull on the velic traverse, and that also allows directional control. Thus, rather than considering the OPI as a single sphincter, perhaps a more apt characterization of the OPI is as a complex structure that may be differently constricted using multiple distinct mechanisms. As we have shown, each such mechanism has its own dedicated muscular structure, and each is specialized to generate a particular, reliable outcome (e.g., a uvular fricative or a uvular vowel). Structures of this kind are consistent with Loeb et al's. (2000) definition of "robust muscle synergies", being biomechanically effective modular neuromuscular structures (see, e.g., Berniker et al. 2009, Berger et al. 2013) that are both reliable (i.e., robust to activation noise) and localized. Seeking such properties through biomechanical modeling may thus provide researchers with the tools to uncover the neurophysiological primitives that underlie speech (see Gick and Stavness 2013).

While it is essential to include the tongue in our simulations to allow observation of changes in the OPI and to provide passive resistance due to gravity and baseline elasticity, the tongue plays a rather passive role, with no tongue muscles aside from PG activated. That said, the present study has established a basis from which future work may more deeply explore the role of the tongue. In particular, the complete OPI closure that was not effected in Figure 6 should presumably be easily achieved with more active raising and backing of the tongue; likewise, lateral bracing of the tongue (e.g., Stone 1990) in different locations and configurations would, in combination with the actions of the PG and PP described here, provide a variety of distinct mechanisms for reliably producing OPI constrictions of varying sizes and shapes. Other future improvements to our numerical model will include using improved muscle models, geometry based on a single, unified subject and segmentation process, a less course discretization, and further validation against speech production data (using endoscopy, ultrasound, x-ray, x-ray microbeam, and MRI).

Acknowledgements

The authors thank A. Ho for assistance with simulations, A. Klenin for assistance with figure preparation, and S. Bird and S. Moisik for helpful discussion.

Funding

This work was supported by a Discovery Grant to the first author from the Natural Sciences and Engineering Research Council of Canada and by NIH Grant DC-002717 to Haskins Laboratories.

References

Bell-Berti F, Hirose H. Patterns of palatoglossus activity and their implications for speech organization. Haskins Labs. Status Report on Speech Res. 1973; 34:203–209.

Bell-Berti F. An electromyographic study of velopharyngeal function in speech. J. Speech Hear. Res. 1976; 19:225–240. [PubMed: 979198]

Benguerel AP, Hirose H, Sawashima M, Ushijima T. Velar coarticulation in French: An electromyographic study. J. Phonet. 1977; 5:157–167.

Berger DJ, Gentner R, Edmunds T, Pai DK, d'Avella A. Differences in adaptation rates after virtual surgeries provide direct evidence for modularity. J. Neurosci. 2013; 33:12384–12394. [PubMed: 23884944]

Berniker M, Jarc A, Bizzi E, Tresch MC. Simplified and effective motor control based on muscle synergies to exploit musculoskeletal dynamics. Proc. of the National Acad. of Sci., USA. 2009; 106:7601–7606.

Berry DA, Moon JB, Kuehn DP. A finite element model of the soft palate. Cleft Pal. Craniofac. J. 1999; 36:217–223.

Campos D, Ellwanger JH, Costa Rosa JP, Santos IP, Silva TH, Piazza JL, Kraether Neto L. Palatoglossus muscle neuroanatomy - a review. J. Morphol. Sci. 2012; 29:123–124.

Chen H, Fels S, Pang T, Tsou L, Almeida F, Lowe AA. Three-dimensional reconstruction of soft palate modeling from subject-specific magnetic resonance imaging data. Sleep and Breathing. 2012; 16:1113–1119. [PubMed: 22057794]

Cui L, Perreault EJ, Maas H, Sandercock TG. Modeling short-range stiffness of feline lower hindlimb muscles. J. Biomech. 2008; 41:1945–1952. [PubMed: 18499113]

Dantas RO, Dodds WJ, Massey BT, Shaker R, Cook IJ. Manometric characteristics of glossopalatal sphincter. Digest. Diseases & Sci. 1990; 35:161–166. [PubMed: 2302972]

Ettema SL, Kuehn DP, Perlman AL, Alperin N. Magnetic resonance imaging of the levator veli palatini muscle during speech. Cleft Pal. Craniofac. J. 2002; 39:130–144.

Faber C. Tobacco smoking in relation to lung disease. Half-yearly Compendium of Medical Science, Pt. XXII. 1878:113–115.

Fritzell B. The velopharyngeal muscles in speech: An electromyographic and cineradiographic study. Acta Oto-laryngol. Suppl. 1969; 250:1–81.

Fritzell B. Electromyography in the study of the velopharyngeal function-a review. Folia Phoniat. 1979; 31:93–102. [PubMed: 488874]

Fujimura O. Comments on "On the Quantal Nature of Speech", by K. N. Stevens. J. Phonet. 1989; 17:87–90.

Gerard, JM.; Perrier, P.; Payan, Y. 3D biomechanical tongue modelling to study speech production. In: Harrington, J.; Tabain, M., editors. Speech Production: Models, Phonetic Processes and Techniques. New York: Psychology Press; 2006. p. 85-102.

Gick B, Francis N, Klenin A, Mizrahi E, Tom D. The velic traverse: an independent oral articulator? J. Acoust. Soc. Am. 2013; 133:EL208–EL213. [PubMed: 23464130]

Gick B, Stavness I. Modularizing speech. Front. Psychol. 2013; 4:977. [PubMed: 24399989]

Gick B, Stavness I, Chiu C, Fels SS. Categorical variation in lip posture is determined by quantal biomechanical-articulatory relations. Can. Acoust. 2011; 39:178–179.

Huang YQ, White DP, Malhotra A. The impact of anatomic manipulations on pharyngeal collapse: results from a computational model of the normal human upper airway. Chest. 2005; 128:1324–1330. [PubMed: 16162725]

Korioth TW, Hannam AG. Deformation of the human mandible during simulated tooth clenching. J. Dent. Res. 1994; 73:56–66. [PubMed: 8294619]

Kuehn DP, Azzam NA. Anatomical characteristics of palatoglossus and the anterior faucial pillar. Cleft Pal. J. 1978; 15:349–359.

Kuehn DP, Folkins JW, Cutting CB. Relationships between muscle activity and velar position. Cleft Pal. J. 1982; 19:25–35.

Liu ZS, Luo XY, Lee HP, Lu C. Snoring source identification and snoring noise prediction. J. Biomech. 2007; 40:861–870. [PubMed: 16737702]

Loeb E, Giszter SF, Satiel P, Mussa-Ivaldi FA, Bizzi E. Output units of motor behavior: An experimental and modeling study. J. Cogn. Neurosci. 2000; 12:78–97. [PubMed: 10769307]

Lubker JF, Fritzell B, Lindqvist J. Velopharyngeal function: An electromyographic study. Spch. Transmission Lab. Quarterly Progress & Status Rep. 1970; 11:9–20.

Lubker, JF.; May, K. Palatoglossus function in normal speech production. Papers from the Instit. of Ling.; Stockholm Univ.. 1973. p. 17-26.

Moon JB, Smith AE, Folkins JW, Lemke JH, Gartlan M. Coordination of velopharyngeal muscle activity during positioning of the soft palate. Cleft Pal. Craniofac. J. 1994; 31:45–55.

Nazari MA, Perrier P, Chabanas M, Payan Y. Shaping by Stiffening: A Modeling Study for Lips. Mot. Control. 2011; 15:141–168.

Peck CC, Langenbach GE, Hannam AG. Dynamic simulation of muscle and articular properties during human wide jaw opening. Arch. Oral Biol. 2000; 45:963–982. [PubMed: 11000383]

Perry JL. Anatomy and physiology of the velopharyngeal mechanism. Seminars in Speech and Lang. 2011; 32:83–92.

Seaver EJ III, Kuehn DP. A cineradiographic and electomyographic investigation of velar positioning in non-nasal speech. Cleft Pal. J. 1980; 17:216–226.

Serrurier A, Badin P. A three-dimensional articulatory model of the velum and nasopharyngeal wall based on MRI and CT data. J. Acoust. Soc. Am. 2008; 123:2335–2355. [PubMed: 18397037]

Stavness I, Gick B, Derrick D, Fels SS. Biomechanical modeling of English /r/ variants. J. Acoust. Soc. Am. 2012; 131:EL355–EL360. [PubMed: 22559452]

Stavness I, Lloyd J, Payan Y, Fels S. Coupled hard-soft tissue simulation with contact and constraints applied to jaw-tongue-hyoid dynamics. Int. J. of Num. Meth. in Biomed. Eng. 2011; 27:367–390.

Stone M. A three-dimensional model of tongue movement based on ultrasound and x-ray microbeam data. J. Acoust. Soc. Am. 1990; 81:2207–2218. [PubMed: 2189921]

Takano S, Honda K. An MRI analysis of the extrinsic tongue muscles during vowel production. Speech Communication. 2007; 49:49–58.

Wang Y, Wang J, Liu Y, Yu S, Sun X, Li S, Shen S, Zhao W. Fluid-structure interaction modeling of upper airways before and after nasal surgery for obstructive sleep apnea. Int. J. Num. Meth. in Biomed. Eng. 2012; 28:528–546.

Zajac FE. Muscle and tendon: properties, models, scaling, and application to biomechanics and motor control. Crit. Reviews in Biomed. Eng. 1989; 17:359.

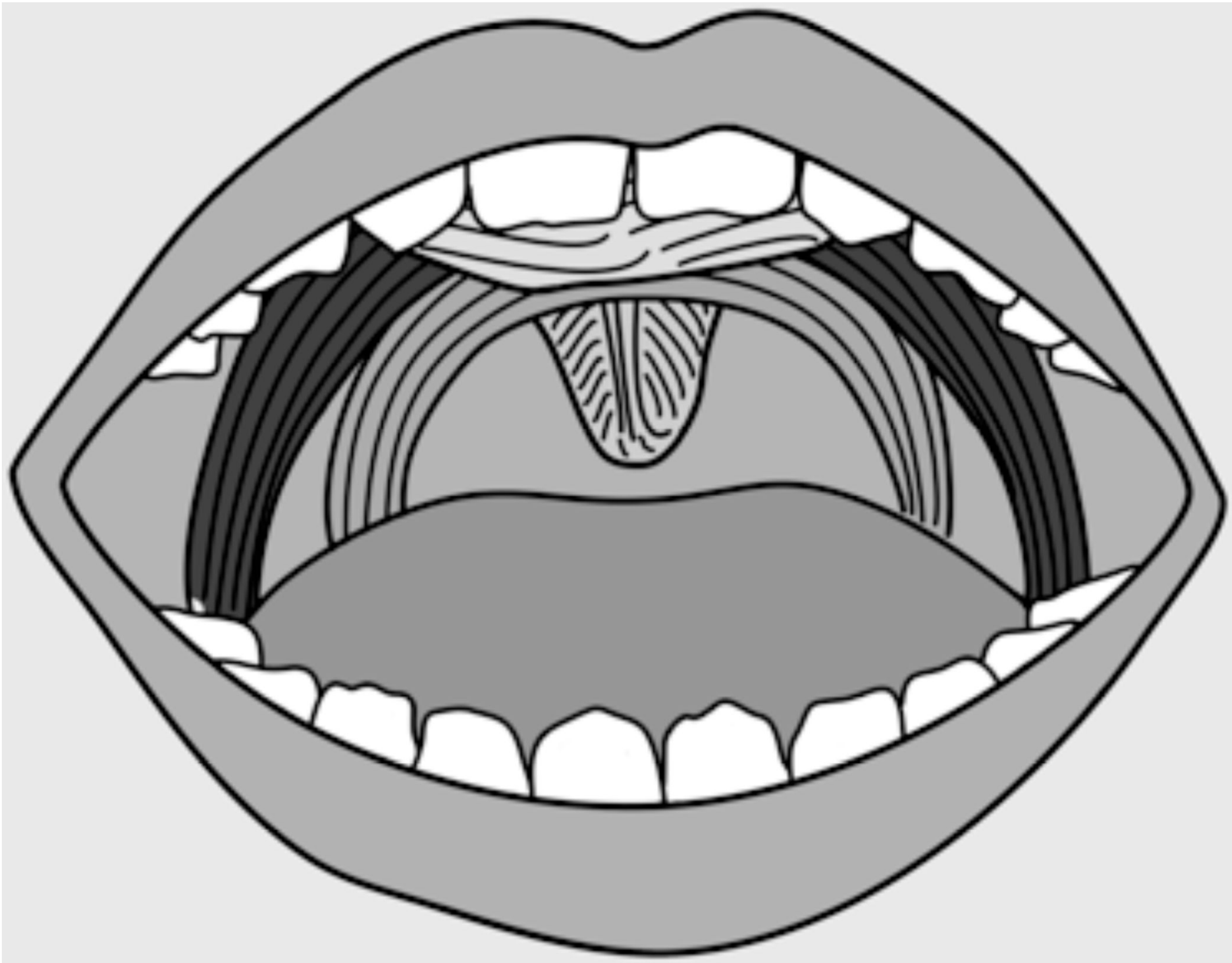

Figure 1.
Schematic image of the structures of the OPI, showing the tongue (below), the palate (above), and the anterior (dark gray) and posterior (light gray) faucial pillars.

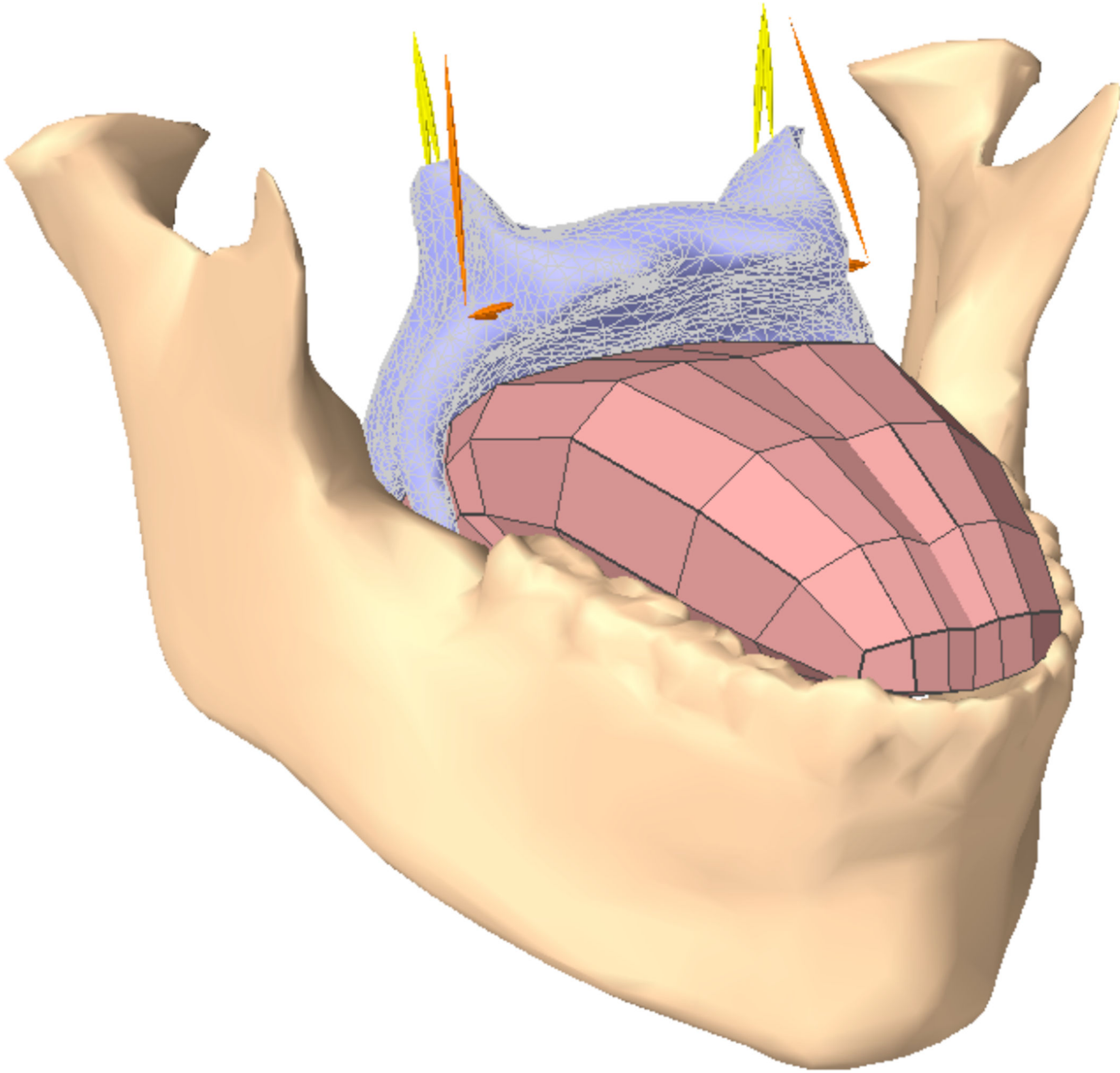

Figure 2.
Oblique anterior overview of the Jaw–Tongue–Hyoid–Soft palate model.

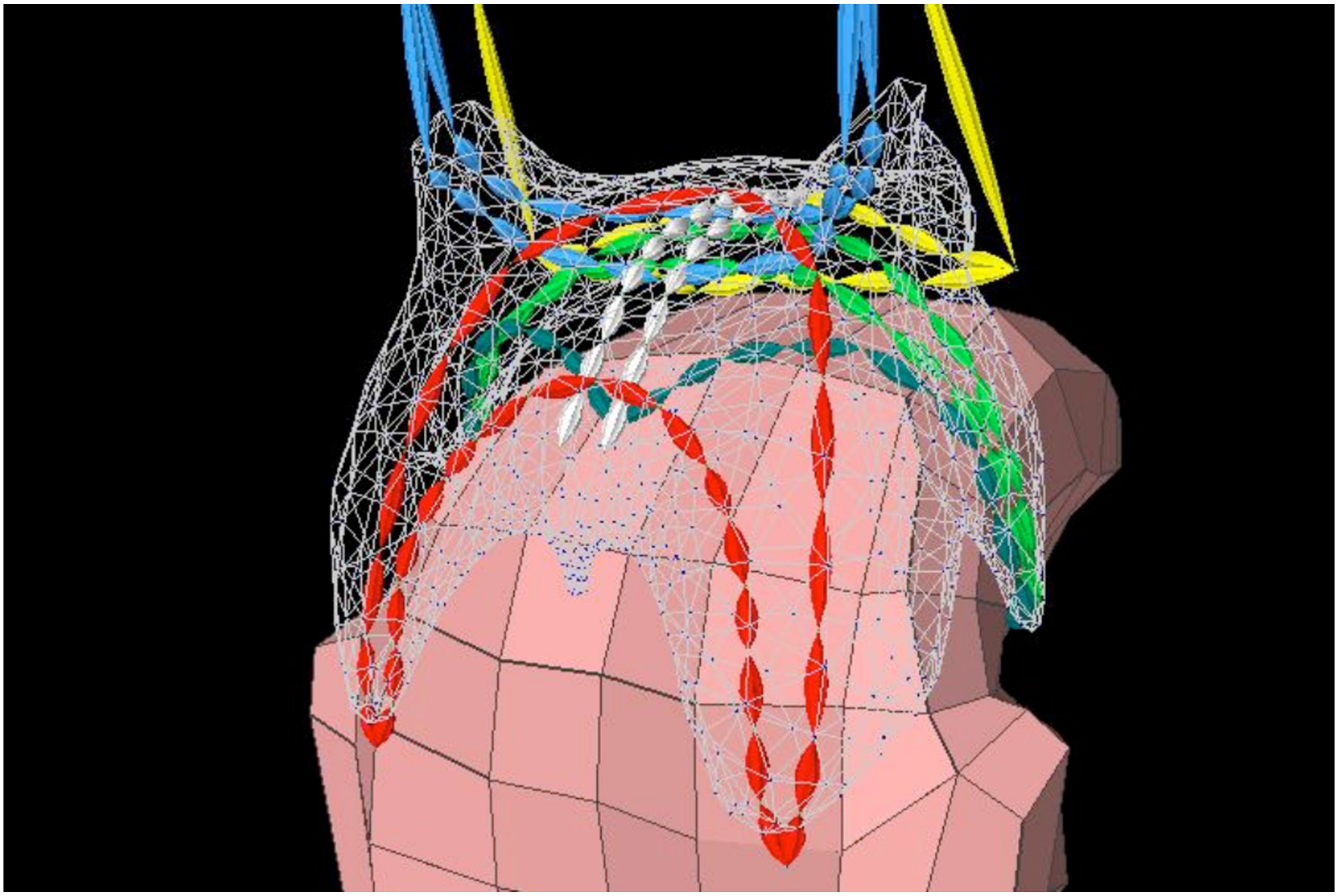

Figure 3.

Oblique posterior view of the soft palate model, with muscle paths shown for PGa (light green) PGp (dark green), palatopharyngeus (red), musculus uvulae (white), tensor veli palatini (yellow), and levator veli palatini (blue).

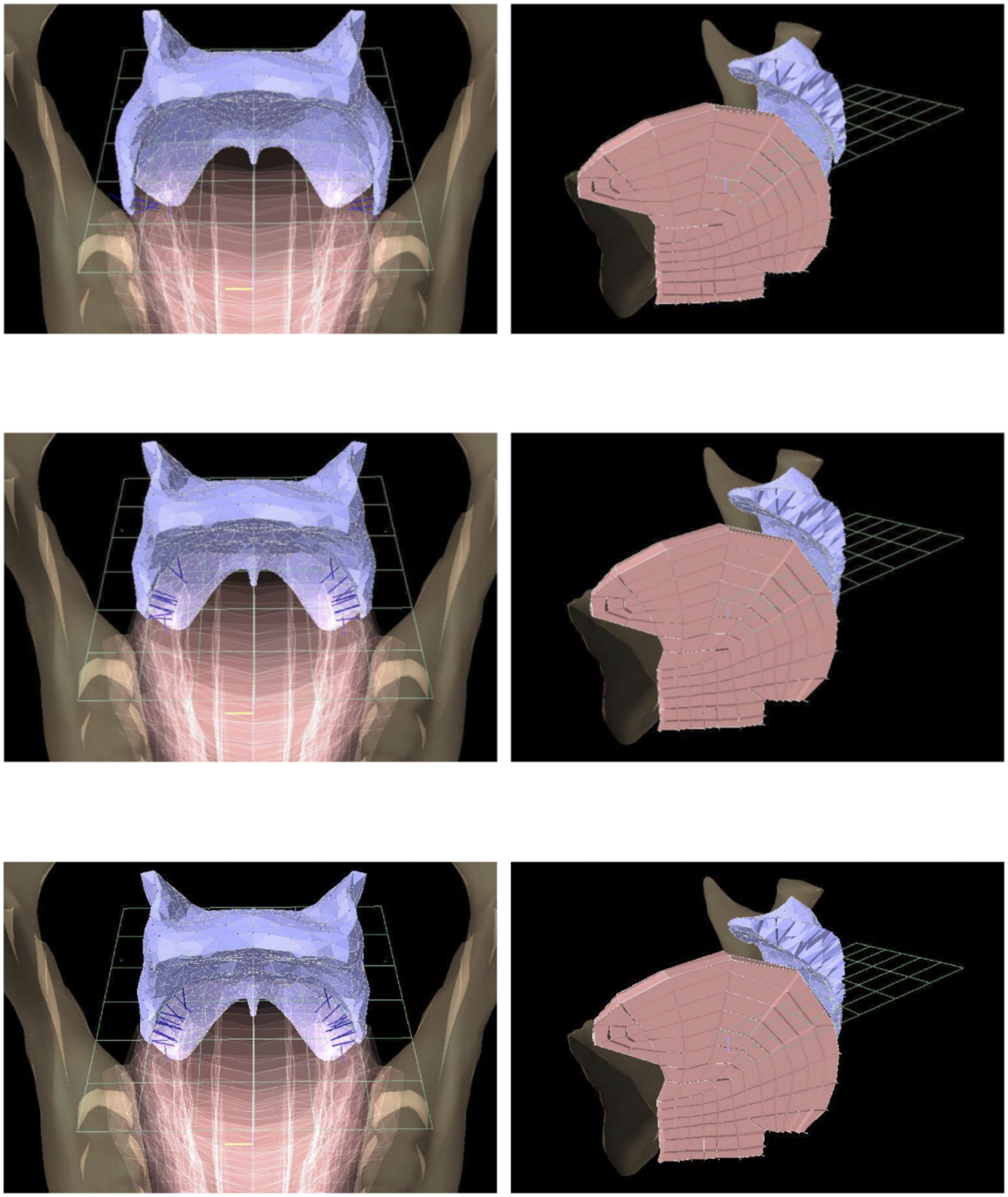

Figure 4.

Effect of the PG muscle (anterior + posterior) on OPI constriction, shown in anterior bird's-eye view (left column) and midsagittal cutaway view (right column). The images in (a) (top row) are taken immediately before muscle activation, (b) (middle row) shows the mid-point of the movement, and (c) (bottom row) is taken at the end of muscle activation. Short, dark blue line segments along the tongue edge indicate normal vectors at contact points between the tongue and soft palate. The grid visible in these images intersects the model through the measurement plane used to measure OPI area; grid squares are 1 cm^2.

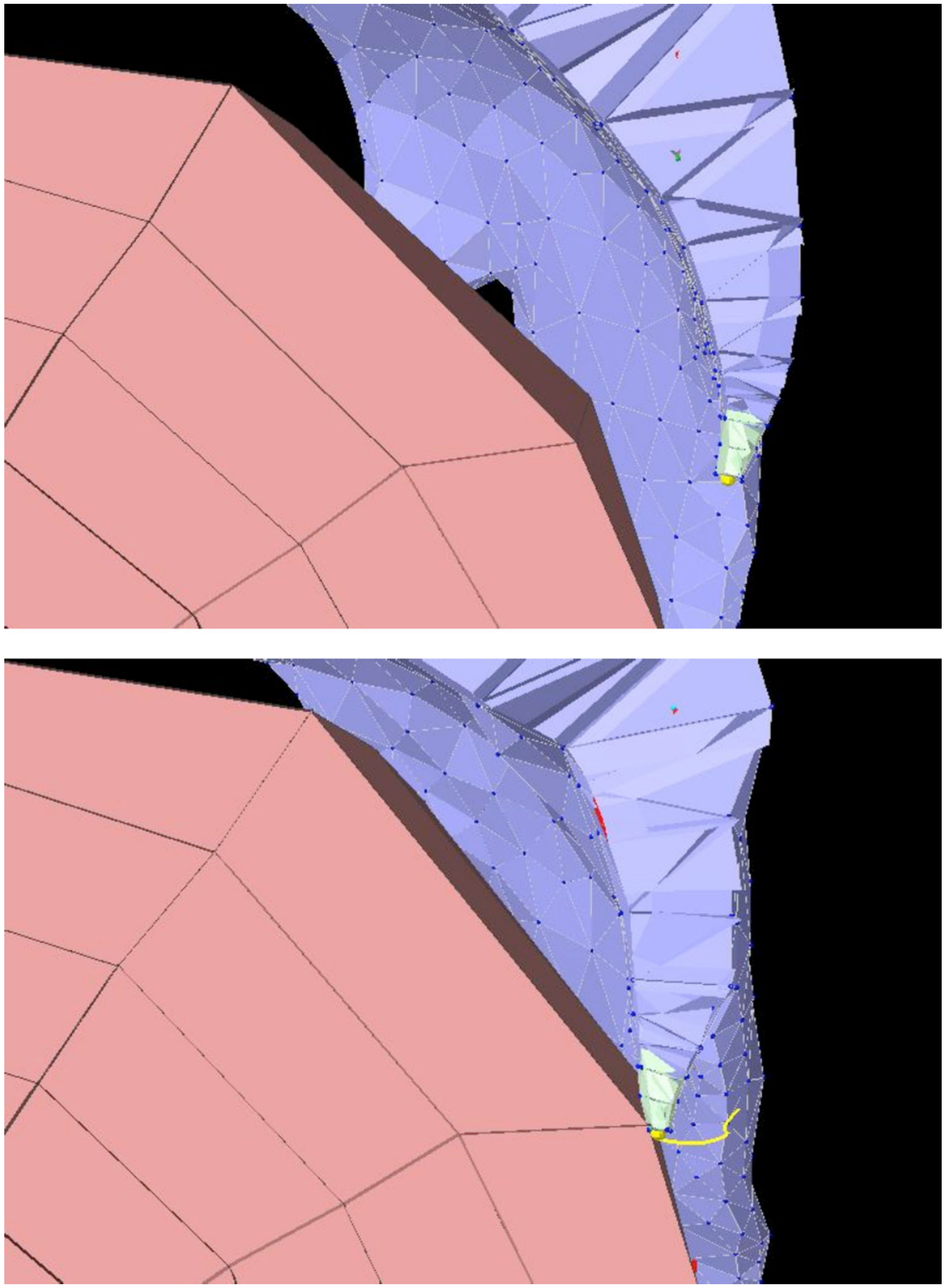

Figure 5.

Action of the posterior PG muscle on the uvula; the tip of the uvula is shown in light green; yellow tracing shows the path of the tip of the uvula. Image (a) is taken immediately before muscle activation, (b) shows contact between the uvula and the tongue.

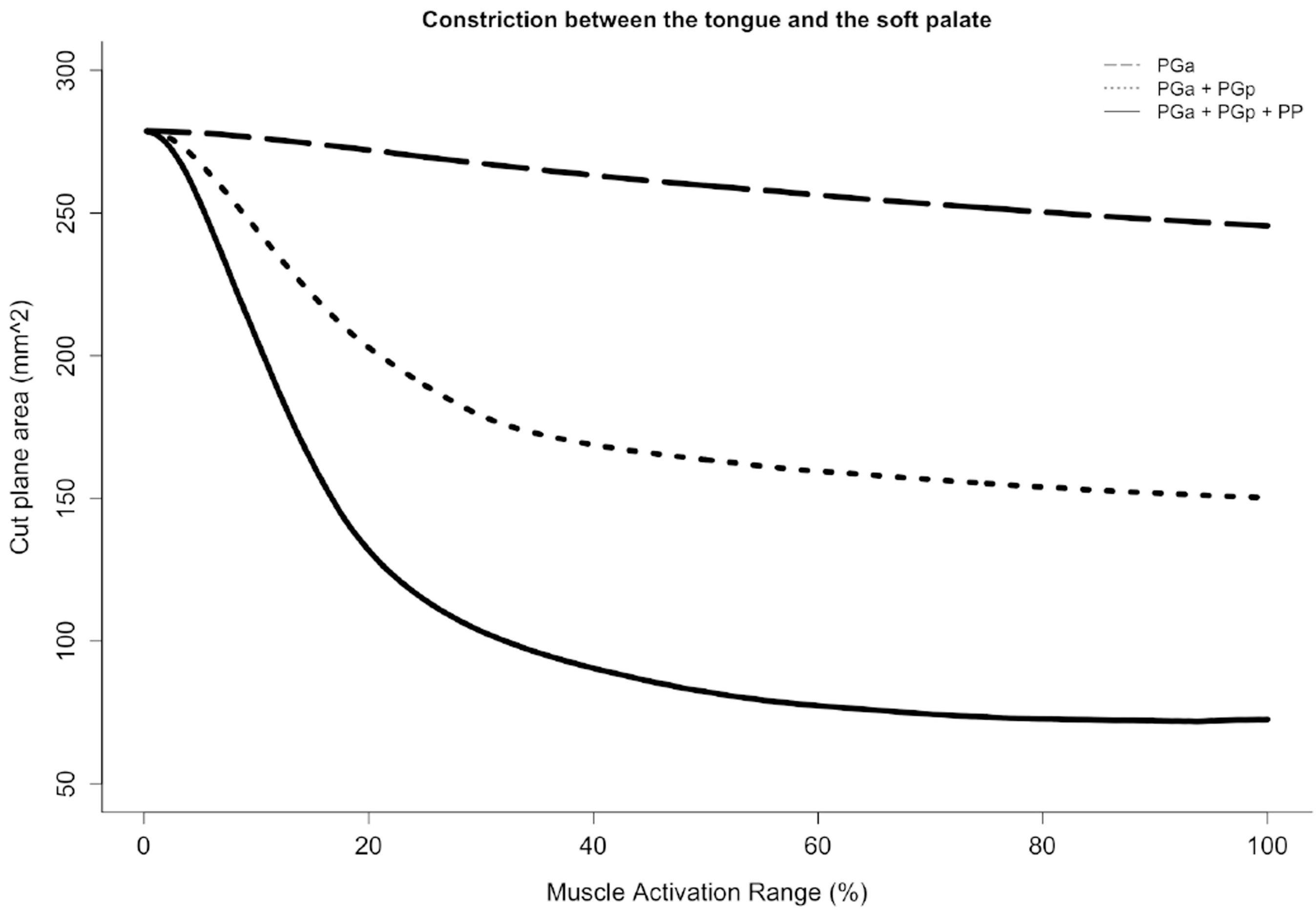

Figure 6.

OPI intersect plane area, with the dashed line showing activation of PGa, dotted line showing PGa + PGp, and solid line showing PGa + PGp + PP.